Polym. Bull. (2012) 68:507–528
DOI 10.1007/s00289-011-0634-5

ORIGINAL PAPER

Modeling of kinetics of pertechnetate removal by amino-functionalized glycidyl methacrylate copolymer

Danijela D. Maksin · Radmila V. Hercigonja · Magdalena Ž. Lazarević · Marija J. Žunić · Aleksandra B. Nastasović

Received: 27 June 2011 / Revised: 17 September 2011 / Accepted: 18 September 2011 /
Published online: 30 September 2011

Abstract Technetium-99 comprises a significant health risk, since edible plants can bioaccumulate and convert it to more lipophilic species that cannot be excreted through urine. Batch kinetics of pertechnetate removal from aqueous solutions by two samples of crosslinked poly(glycidyl methacrylate-*co*-ethylene glycol dimethacrylate) functionalized with diethylene triamine (PGME-deta) was investigated at the optimum pH value of 3.0, and the initial solution activity of 325 MBq dm^{-3}. PGME-deta was characterized by elemental analysis, mercury intrusion porosimetry, and scanning electron microscopy. Five kinetic models (pseudo-first, pseudo-second order, Elovich, Bangham, and intraparticle diffusion) were used to determine the best-fit equation for pertechnetate sorption. After 24 h, PGME-deta samples sorbed more than 98% of pertechnetate present, with maximum sorption capacity of 25.5 MBq g^{-1}, showing good potential for remediation of slightly contaminated groundwater.

D. D. Maksin (✉) · M. Ž. Lazarević
University of Belgrade, Vinča Institute of Nuclear Sciences, P.O. Box 522, 11000 Belgrade, Republic of Serbia
e-mail: dmaksin@vinca.rs; dmaksin@gmail.com

R. V. Hercigonja
Faculty of Physical Chemistry, University of Belgrade, Studentski trg 12-14, 11000 Belgrade, Republic of Serbia

M. J. Žunić
University of Belgrade, ICTM-Center for Catalysis and Chemical Engineering, Njegoševa 12, 11000 Belgrade, Republic of Serbia

A. B. Nastasović
University of Belgrade, ICTM—Center for Chemistry, Polymer Department, Studentski trg 12-16, 11000 Belgrade, Republic of Serbia

Keywords Pertechnetate · Sorption kinetics · Macroporous copolymer · Amino-functionalized

Introduction

Technetium-99 (^{99}Tc) is among the most abundant constituents of long half-life nuclear waste, since it has a high production rate in the fission of ^{235}U and ^{239}Pu (product yield of 6.1 and 6.2%, respectively) [1]. ^{99}Tc also occurs naturally in very small amounts in the earth's crust. It is a long-lived radionuclide (soft β-emitter, with $E_{max} = 294$ keV) (1 electron volt, eV $= 1.6022 \times 10^{-19}$ joules, J) with a half-life of 2.13×10^5 years, which ensures its long-term presence in nature, once released. A significant amount of ^{99}Tc has been let out into the environment during the last few decades through the detonation of nuclear weapons (especially atmospheric weapons tests), nuclear reactor airborne emissions, nuclear fuel reprocessing plant airborne emissions, and by improper discharges from facilities that treat or store radioactive waste. It is considered to be an important contributor to the future collective dose to the population due to the use of nuclear energy [2].

Under typical oxic conditions in the environment, ^{99}Tc forms the pertechnetate anion (TcO_4^-) which is quite soluble (11.3 mol dm^{-3}, at 273 K, for sodium salt) and mobile in groundwater. It is the predominant aqueous species over the complete pH range of natural waters [3]. TcO_4^- is only slightly sorbed by most sediments under oxidizing conditions [4]. Tc(VII) can be reduced to Tc(IV) by biotic and abiotic processes in soil, which usually results in immobilization [5]. Pertechnetate sorption has been positively correlated with the organic carbon content in the soil [6]. However, this sorbed technetium is remobilized as soon as the soil is exposed to air and water [7]. The pertechnetate anion comprises a significant health risk because it easily enters the food chain. Even though TcO_4^- by itself is not human health hazard if ingested, since it is easily excreted through urine, many plant forms and various aquatic life bioaccumulate TcO_4^-, metabolizing it to produce more lipophilic forms which are retained in the body, analogously to what is observed in the case of mercury uptake [8]. This combination of chemistry and biology make the pertechnetate anion an especially dangerous radioactive pollutant.

EPA has established a maximum contaminant level (MCL) of 0.04 mSv per year for β and γ radioactivity from man-made radionuclides, including ^{99}Tc, in drinking water [9]. The average concentration of ^{99}Tc which is assumed to yield 0.04 mSv per year is 33.3 Bq dm^{-3}. Since this regulation states that the sum of the annual dose from all artificial β and γ emitters shall not exceed 0.04 mSv, the amount of ^{99}Tc which is allowed to be released is considerably smaller.

Diverse natural and synthetic materials have been investigated for their potential use for removal of ^{99}Tc from the environment. TcO_4^- can be strongly sorbed on stibnite [10], pyrrhotine, pyrite and magnetite [11], elemental iron [12], organophilic bentonites [13], activated carbon [14–16], various synthetic resins, and sponges [17–21].

Aside from the application of these nonspecific materials, lately there has been significant progress in molecular recognition of pertechnetate and perrhenate anions, through highly specific synthetic receptors [22].

Macroporous hydrophilic copolymers based on glycidyl methacrylate, GMA, synthesized by radical suspension copolymerization in the shape of regular beads of desired size, with required porosity parameters, have been successfully employed in the separation and concentration of heavy and precious metals, owing to their high capacity, fast kinetics and good selectivity, combined with chemical and mechanical stability. The epoxy group in GMA molecule is used for introduction of various functional groups: amino, hydroxyl, iminodiacetate, thiol, dithiocarbamate, azole etc. Amino-functionalized glycidyl methacrylate copolymers can be prepared by the reaction of the epoxy groups of the copolymer with compounds containing primary amino groups [23–25] etc. The advantage of such copolymers over the conventional ion-exchange resins lies in the fact that, depending on pH, they can both coordinate heavy and precious metals and, acting as basic ion exchangers, bind them as chloro complexes [9]. This led us to believe that these copolymers may be amenable for use for anion sorption. In our previous research, we have successfully employed amino-functionalized copolymers for the removal of Cr(VI) anionic species from acidic solutions [23]. Kim et al. [26] demonstrated that ReO_4^-, which is often used as pertechnetate analog, is efficiently sorbed by natural organic polymer chitosan containing amino groups, while Plevaka et al. [27] showed that perrhenate binds to fibrous chitosan-carbon materials. In the case of Forager sponges which contain both amino and carboxylic groups [28], it was suggested that pertechnetate sorption occurs probably through amine-containing functional groups [17]. On the basis of this research, we concluded that amino-functionalized copolymers may be used for pertechnetate sorption.

In this study, kinetics of pertechnetate sorption was investigated using two samples of macroporous crosslinked poly(glycidyl methacrylate-*co*-ethylene glycol dimethacrylate), PGME, with different amounts of the crosslinker, functionalized by the ring-opening reaction of epoxy groups with diethylene triamine (abbreviated PGME-deta). Five kinetic models (the pseudo-first, the pseudo-second order, Elovich, Bangham, and the intraparticle diffusion model) were used to determine the best-fit equation for pertechnetate sorption. Effectiveness of the sorption process for pollutant removal from aqueous solutions strongly depends on the sorption dynamics. Thus, predicting the rate at which sorption takes place in a given system is one of the crucial factors in sorption system design [29]. As far as we are aware, there is a marked lack of literature regarding modeling the dynamics of ^{99}Tc removal.

In order to provide accurate and efficient measurements of sorbed ^{99}Tc with minimal exposure, sorption experiments were performed using $^{99m}TcO_4^-$ anion containing ^{99m}Tc isotope, since technetium-99m is regarded as chemically equivalent to technetium-99 [16]. ^{99m}Tc is a metastable nuclear isomer of ^{99}Tc, which emits readily detectable 140 keV γ rays and its half-life for monoenergetic γ emission is 6.0058 h. ^{99m}Tc undergoes an isomeric transition to yield ^{99}Tc: $^{99m}Tc \rightarrow {}^{99}Tc + \gamma$.

Experimental

All the chemicals used were analytical grade products and used as received: glycidyl methacrylate (GMA) (Merck), ethylene glycol dimethacrylate (EGDMA) (Fluka), diethylene triamine (DETA) (Merck), 2,2′-azobisisobutyronitrile (AIBN) (Merck), poly(*N*-vinyl pyrrolidone) (Kollidone 90, BASF), cyclohexanol (Merck), 1-tetradecanol (Merck), and toluene (Merck).

Preparation of PGME-deta copolymers

Two macroporous PGME samples were prepared by a radical suspension copolymerization. The reaction mixture consisted of the monomer phase (75.0 g) containing monomer mixture (19.5 g GMA and 13.0 g EGDMA for sample 1 and 26.0 GMA and 6.5 g EGDMA for sample 2), AIBN as initiator (0.3 g), and 45.2 g of inert component (34.0 g of cyclohexanol and 8.5 g of 1-tetradecanol), which was suspended in the aqueous phase consisting of 225.0 g of deionized water and 2.25 g poly(*N*-vinyl pyrrolidone). The copolymerization was carried out at 343 K for 2 h and at 353 K for 6 h with a stirring rate of 300 rpm. After the completion of the reaction, the copolymer particles were washed with water and ethanol, kept in ethanol for 12 h and dried in vacuum at 313 K. The synthesized samples were purified by Soxhlet extraction with ethanol for 24 h. The fraction of the resulting crosslinked beads with the average particle diameter (D) in the range of 150–300 μm was separated by sieve analysis and used for amino-functionalization and sorption experiments.

The synthesized PGME samples were functionalized with diethylene triamine using the following procedure. A mixture of 7.2 g of copolymer sample, 31.4 g of diethylene triamine, and 300 cm^3 of toluene was left at room temperature for 24 h and then heated for 6 h at 353 K at a stirring rate of 250 rpm. The modified samples were filtered, washed with ethanol, dried, and labeled as PGME1-deta and PGME2-deta (additional label -deta designates functionalization with diethylene triamine).

Characterization of sorbent

The copolymer samples were analyzed for their C, H, and N content using the Vario EL III device (GmbH Hanau Instruments, Germany). Elemental analysis was calculated from multiple determinations within ±0.2% agreement.

The porosity parameters and the specific surface areas of the copolymer samples were determined by a high pressure mercury intrusion porosimeter Carlo Erba Porosimeter 2000, operating in the interval of 0.1–200 MPa. Sample preparation was performed at room temperature and pressure of 0.5 kPa. Samples were outgassed at 323 K and 1 mPa for 6 h. Mean porosimetry curves were acquired from triplicate measurements.

Surface and interior morphology of the PGME-deta beads was investigated by a scanning electron microscope (SEM; JEOL, JSM-6460 LV, Tokyo, Japan). Multiple images were recorded.

Sorption experiments

Preliminary investigations with the aim to establish the pH dependence of $^{99m}TcO_4^-$ sorption and determine the optimum pH for kinetic studies were performed by monitoring ^{99m}Tc uptake in the pH range of 1–14, using appropriate buffer solutions [31], prepared from reagent-grade chemicals. A pH meter, Beckman F40 with a combined Ag/AgCl electrode, was employed for adjusting pH values.

$^{99m}TcO_4^-$ sodium solution was eluted from $^{99}Mo/^{99m}Tc$ generator (Vinča Institute of Nuclear Sciences), and uptake of $^{99m}TcO_4^-$ from aqueous solutions by the amino-functionalized copolymer samples was monitored at room temperature in static (batch) experiments. The same mass of each sample (50 mg) was contacted with 1 cm^3 of ^{99m}Tc-pertechnetate aqueous solution and 3 cm^3 of the appropriate buffer solution. The pH of the sorbate solution was varied from 1.0 to 14.0. For each pH value, a blank without copolymer was prepared in the same manner. After 90 min, 180 min, and 24 h, 0.100 cm^3 aliquots were removed and their activity measured.

The sorption dynamics data was subsequently collected at the selected pH value, by measuring residual radioactivity in supernatant solution, following the procedure described above, after 5, 30, 60, 90, 180 min and 24 h.

All the uptake experiments were conducted in triplicate, and sometimes repeated again, and the mean values have been reported. Standard errors for percent uptake calculated from triplicate measurements were less than or equal to 4.1%.

Measurement of emission

Unlike α and β particles which have relatively short ranges even in air, γ rays are electromagnetic radiation of high frequency, naturally produced on Earth by decay of high energy states in atomic nuclei. Gamma rays have the smallest wavelengths and the most energy of any other wave in the electromagnetic spectrum. Difficulties associated with α and β radiation detection and measurement (scattering from the source surface, self-absorption and absorption in the source sheathing, absorption of radiation in the counter window and housing etc.) [30] are minimized or altogether avoided when γ rays are detected and measured. Also, γ radiation detection enables energy selective counting (α and β are not monoenergetic).

The weak β emission, such as emitted by ^{99}Tc is stopped by the walls of laboratory glassware. Therefore, it is advisable to perform activity measurements utilizing a more suitable technetium radioisotope, like ^{99m}Tc which decays by isomeric transition to its ground state with the emission of a 140.5-keV γ ray.

The specific activity of pertechnetate eluate was determined by a Capintec CRC-15β dose calibrator (well-type NaI(Tl) scintillation detector; filled with pressurized 99% Ar gas $\sim$ 200 kPa) and adjusted by adding saline solution to 1.3 MBq cm^{-3}. Activity measurements were executed by placing a glass vial containing pertechnetate solution into a $4\pi\gamma$-ionization chamber of the instrument (Pb shielded from background radiation, natural or parasitic) and reading the activity of the selected radionuclide, i.e., ^{99m}Tc on the display. Calibration and verification before each set of measurements is performed using ^{137}Cs and ^{60}Co radioisotopes.

All ^{99m}Tc supernatant analyses were carried out using a $2\pi\gamma$-solid-state scintillation detector (LKB Wallac 1282 Compugamma, Finland) with autosampler, which makes use of a well-type single crystal of thallium-activated sodium iodide. All measurements were performed with reference to a sample (0.100 cm^3) of the initial ^{99m}Tc solution adjusted to appropriate pH at the start of experiment, to allow the conversion of counts per minute (cpm) to percent uptake.

Relative measurements of sorbed radioactivity were obtained using the following equation:

$$R = \frac{R_b - R_s}{R_b} \cdot 100\%$$

where R is the sorbed pertechnetate activity (%), R_b is the measured activity of the reference or blank aliquot (cpm) for a given pH, and R_s is the activity of the supernatant aliquot (cpm) for the same pH value. Since equal volumes of both reference solution and supernatant samples were counted under the same conditions, all geometry and background considerations cancelled out, and it was not necessary to calculate corrected cpm values. Self-absorption has no effect in γ counting in which the sample volume is small. Coated tubes used for sample introduction into the instrument do not suffer from self-absorption. The volume of coated surface is too small to attenuate γ radiation.

Samples were counted for 30 s to measure optimum cpm values, with low counting errors. Counting errors were typically less than 10%, due to statistical nature of γ decay.

Daily calibration and instrument check before each set of measurements was performed using ^{129}I radioisotope.

Results and discussion

Synthetic aspects

Two samples of macroporous crosslinked poly(GMA-*co*-EGDMA), with 40 mass% (sample 1) and 20 mass% of EGDMA crosslinker (sample 2), were synthesized via suspension copolymerization in the presence of inert component. The copolymer structure is presented in Scheme 1.

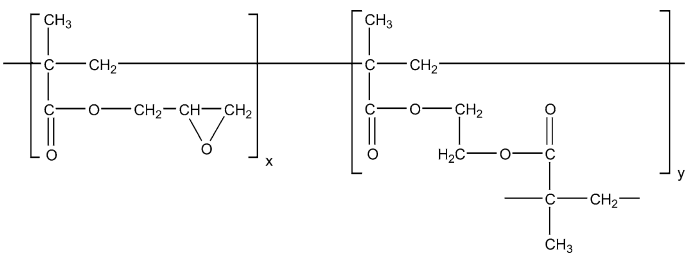

Scheme 1 Chemical structure of poly(GMA-*co*-EGDMA) ($x = 0.60$,y $= 0.40$ for sample 1; $x = 0.80$, $y = 0.20$ for sample 2)

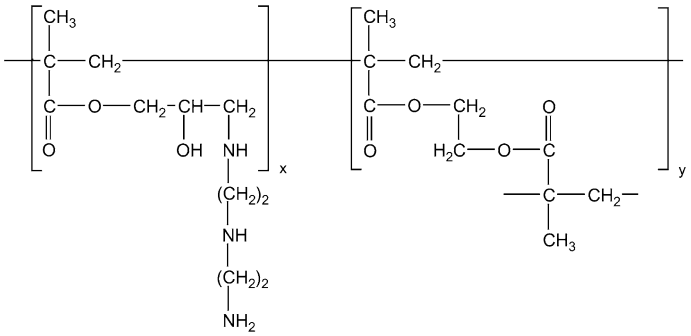

Scheme 2 Chemical structure of amino-functionalized poly(GMA-*co*-EGDMA)-deta ($x = 0.60$, $y = 0.40$ for sample 1-deta; $x = 0.80$, $y = 0.20$ for sample 2-deta)

The initial samples were further amino-functionalized by ring-opening reaction of the pendant epoxy group with diethylene triamine yielding resultant chelating copolymer with hydrophilic character. The amino-functionalized copolymer structure is presented in Scheme 2.

Characterization of PGME-deta samples

The elemental analysis data for PGME-deta samples showed that the conversion of epoxy groups for sample 1-deta of approximately 40% (39.5 ± 0.2% for 1-deta and 38.6 ± 0.2% for 2-deta) is in accordance with our previous results [23, 31]. Sample 2-deta has a somewhat higher ligand concentration (2.17 ± 0.005 mmol g^{-1} as opposed to 1.67 ± 0.004 mmol g^{-1} for 1-deta) [31]. This might indicate better sorption characteristics of 2-deta.

The porous structure of the sorbents is one of the fundamental features required to achieve good sorption. The use of materials with large pores (macropores) is advantageous in promoting a rapid mass transfer that improves the dynamics of sorption. The pore size distribution in macroporous polymers can be controlled by different variables, such as the type of porogen, the polymerization temperature, the amount of porogen solvent and crosslinking monomer, the type and percentage of the initiator [32], and amination conditions [33].

The properties of the pores and the accessibility of the pore volume were investigated by mercury intrusion porosimetry. This technique is suitable for materials containing larger pores (pore diameter range 3 nm–200 μm) [34]. The differential pore size distribution profiles for PGME-deta samples are shown in Fig. 1.

By changing the amount of the crosslinker, EGDMA, (40 mass% for sample 1 and 20 mass% for sample 2 synthesis), macroporous structures with different porosity parameters were obtained (specific surface area, S_{Hg}, specific pore volume, V_S, diameter which corresponds to half of the pore volume, $d_{V/2}$, and average pore diameter, d_P).

The pore size distributions for samples 1-deta and 2-deta are unimodal with maximums which correspond to the most frequent pore diameters. Pore diameters

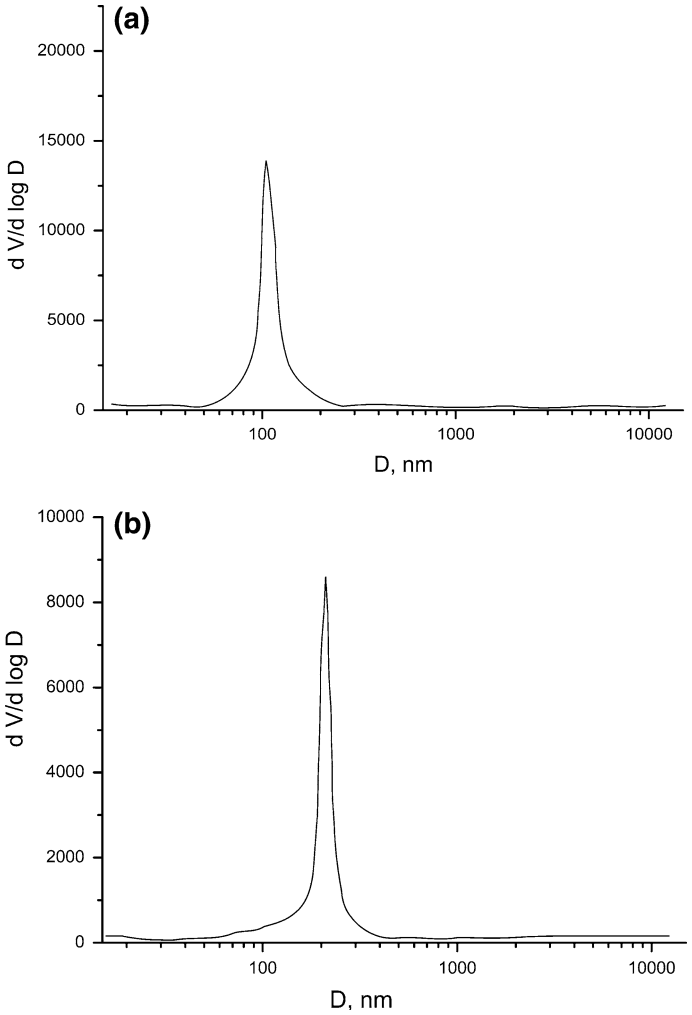

Fig. 1 Differential pore size distribution profiles determined by mercury intrusion porosimetry of 1-deta (**a**) and 2-deta (**b**)

$d_{V/2}$ (107 ± 1.3 nm for 1-deta and 212 ± 2.7 nm for 2-deta) and d_P (96 ± 0.5 nm for 1-deta and 184 ± 1.4 nm for 2-deta) [31] demonstrate that macroporous (diameter > 30 nm) and super-macroporous (diameter > 100 nm) structures account for most of the pores within the porous beads. This result indicates that the beads possess high permeability, which is very favorable for sorption dynamics.

Sample 1-deta has S_{Hg} of 55 ± 0.3 $m^2\ g^{-1}$, approximately twice the size of S_{Hg} of sample 2-deta (29 ± 0.2 $m^2\ g^{-1}$), which suggests possibly enhanced sorption capability of 1-deta, even though the pore volumes are comparable (V_S = 0.91 ± 0.006 $cm^3\ g^{-1}$ for 1-deta and 0.89 ± 0.004 $cm^3\ g^{-1}$ for 2-deta) [31].

Microphotographs of bead surface and cross section, presented in Fig. 2, confirm the macroporous structure of the beads. The images reveal the internal structure formed from microglobules agglomerated into larger clusters.

Sorption of $^{99}TcO_4^-$ by PGME-deta

The treatment procedures for radioactive wastes containing Tc-99 must deal with complex issues. One of the strategies is to separate the waste into sludge containing insoluble, high-activity waste (HAW) species as well as nonradioactive solids, and aqueous liquid portions that will contain tank supernatant and water-soluble species (like pertechnetate) derived from HAW sludge washings [35]. Water-soluble, high-activity species contained in the liquid portion, such as $^{137}Cs^+$ and $^{90}Sr^{2+}$, would be further separated and be added to the HAW portion, leaving an aqueous solution that contains low activity waste (LAW) species and a host of other nonradioactive species such as Na^+, K^+, $Al(OH)_4^-$, Cl^-, F^-, NO_3^-, NO_2^-, OH^-, CO_3^{2-}, and organics [36]. The LAW and HAW fractions resulting from these pretreatment steps would then be separately mixed with appropriate glass material and then vitrified for long-term storage, awaiting radioactivity levels to diminish to non-harmful, i.e., until the waste no longer poses an environmental hazard. However, one potentially troublesome radionuclide remaining in the LAW after pretreatment is ^{99}Tc, a considerable fraction of which occurs as pertechnetate, which warrants further treatment.

The period of time waste must be stored depends on the type of waste [37]. Low-level waste with low levels of radioactivity per mass or volume (such as some common medical or industrial radioactive wastes) may need to be stored for only hours, days, or months, while high-level wastes (such as spent nuclear fuel or by-products of nuclear reprocessing) must be stored for thousands of years.

The conditions in the majority of wastes present at the Hanford, Oak Ridge, and Savannah River sites are highly alkaline (pH 11–14) [35, 38].

Another approach is to dissolve solid fuel waste in concentrated nitric acid as part of the PUREX process [39], de facto standard aqueous nuclear reprocessing method for the recovery of uranium and plutonium from used nuclear fuel, based on liquid–liquid extraction ion-exchange, or its modifications [40]. This process renders, in contrast, extremely acidic solutions.

Most of ^{99}Tc present in fuel reprocessing wastes is still currently stored in underground tanks awaiting recovery, to be separated into HAW and LAW streams. During the nuclear waste vitrification process volatilized ^{99}Tc will be trapped by melter off-gas scrubbers and then washed out into caustic solutions. Plans are being contemplated at this time for the disposal of such secondary waste [41].

^{99}Tc can adversely enter groundwater from mismanaged wastes or through leakage from ^{99}Tc waste storage facilities [17, 42]. One of the main waste streams containing ^{99}Tc results from the decontamination of process equipment in uranium enrichment facilities. The concentration of ^{99}Tc in these wastes can be on the order of 3.7 MBq dm^3 [7, 42]. Contaminated groundwater typically contains above background ($\sim$0.37 MBq dm^3) levels of Tc, but three to five orders of magnitude less than a typical raffinate that is generated from the gaseous diffusion plants [17].

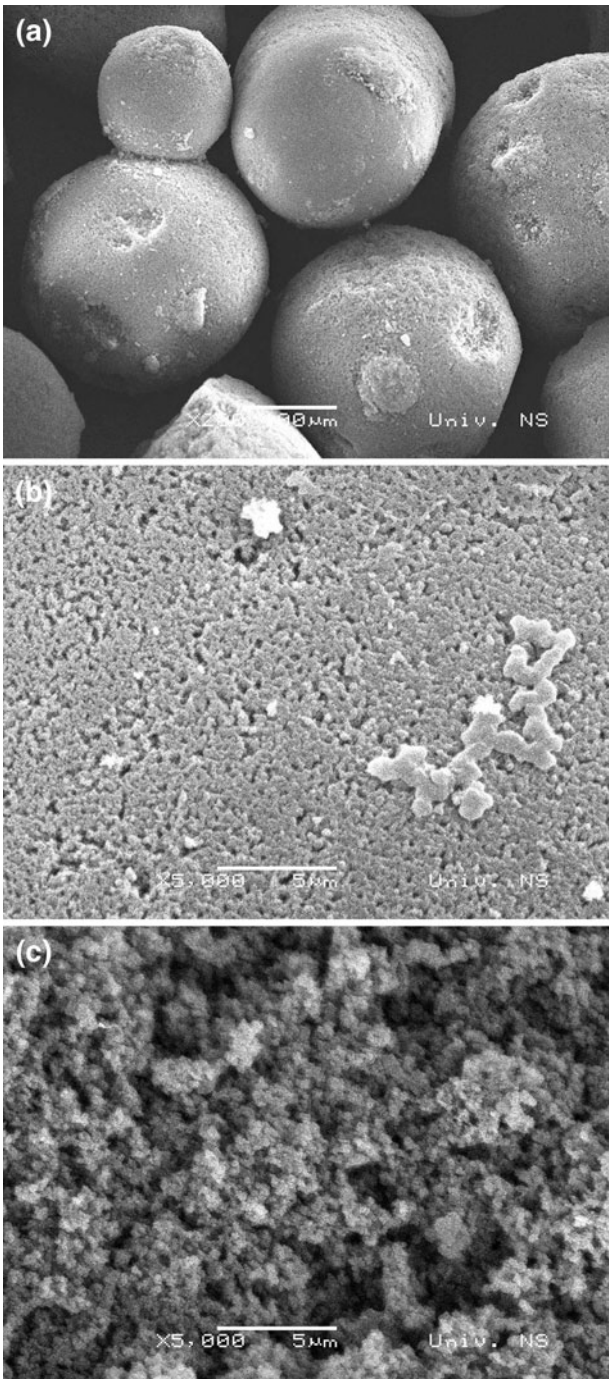

Fig. 2 SEM images of 2-deta beads (×200) (**a**), their surface (×5000) (**b**), and cross section (×5000) (**c**)

Ion exchange is the most common treatment method employed for the treatment of waste streams to remove radioactive contaminants in nuclear facilities [43]. Reliable and effective organic ion-exchange resins are typically used especially in high purity water applications. Weak base resins, which exhibit minimum exchange capacity above a pH of 7.0 [44], are preferred over strong base resins because they require less regenerant chemical, if reuse is the goal.

The ion-exchange process is very effective at transferring the radioactive content of a large volume of liquid into a small volume of solid, which minimizes disposal costs of this secondary waste [43].

Usually it is necessary for the total concentration of salts in solution containing the radionuclide species of interest to be low (<1 g dm^{-3}) [43]. However, the pertechnetate anion is larger and has a lower hydration energy than most of the other anions present in the groundwater in $\sim$4–6 order of magnitude higher concentrations (such as Cl^-, SO_4^{2-}, NO_3^-, and HCO_3^-) [45]. Since small charge-to-size ratio and low-hydration energy are among the factors that increase the affinity of an anion for the resin, there is a natural tendency toward exchanging TcO_4^- preferentially over the other anions in an aqueous solution [46]. This bias can be enhanced by chemical modification of the resin, including varying the type of the cationic exchange sites and the cross-link density of the copolymer [20].

Ion exchange can be implemented in a variety of ways, including in batch systems, column operations, and membrane processes. Batch operation is simple to construct and operate, good for small scale applications, and easily customed for specific treatment problems [43]. Additional advantage is that bead type media are easily removed by filtration.

Regeneration processes are expected to turn out a liquid waste that has higher treatment and disposal costs than the costs saved by a reuse of the media. Also, in theory, ion-exchange process is reversible, but the medium is typically not completely regenerated, with typical restoration rates of up to 90%, i.e., nuclear grade quality is maintained only until the first regeneration [43].

The two main methods for the treatment of spent ion-exchange resins are [43] the destruction of organic compounds to produce inorganic intermediate product that may or may not be further conditioned for storage and/or disposal and direct immobilization, which produces a stable end product. The literature data supports the conclusion that pyrolysis may be an ideal solution for the used ion exchanger, since there seems to be a general consensus that at temperatures $\sim$773 K, the mass percent of solid residue of glycidyl methacrylate-based polymers (barring those containing aromatic substituents) is less than 6% [32, 47, 48].

As already mentioned, PGME-deta copolymer acts as an anion exchanger, under acidic and circumneutral conditions. Primary and secondary amino groups present in its structure, classify it as a weak base ion exchanger.

The interactions between $^{99m}TcO_4^-$ and both PGME-deta resins were examined as a function of the solution pH in the range of 1.0–14.0, since the pertechnetate anion is stable in the complete pH range 1–14, under oxic conditions [3]. Before pH adjustment by the means of buffer solution addition, the pertechnetate saline solution had the pH value of 5. The percent uptake of $^{99m}TcO_4^-$ was measured after

90 min, 180 min, and 24 h, and the pertechnetate uptake data is presented in Table 1.

The pH value of the solution was an important controlling parameter in the sorption process (Table 1). For both investigated copolymers, sorption was inversely correlated with increasing pH. The sorption of pertechnetate is clearly highly favorable, in the wide pH range of 1.0 to 9.0, which is anticipated since pK_a values of the amino groups in weak base anion exchangers are in the range of 8–10. Thus, at pH 8 and above, the number of protonated amino groups decreases, and above 10 their amount becomes negligible. At pH close to 9, a significant number of amino groups become deprotonated. Since the pertechnetate anion is negatively charged, there is no electrostatic attraction to neutral amino groups; the only possible interaction is hydrogen bonding [49]. However, neutral amino groups form intramolecular hydrogen bonds. In addition, at extremely high pH values (>11), there is an abundance of hydroxyl anions present in the solution. Hydrogen bonding of OH^- to the sorbent surface in comparison with TcO_4^- is favored, the overall surface charge becomes negative, which repels the pertechnetate anions, and the sorption becomes immaterial.

As previously stated, there are published studies on rhenium as an analog of radioactive technetium. The findings have shown that, in oxic media, Re(VII) does not interact with anionic functional groups like carboxyl and sulfonate present in organic polymers, and that the crucial factor for noticeable sorption is the presence of amino groups [26, 27]. It is well known that there are two principal means by which anion exchanger can react with anions: chelation and ion exchange. These interactions are described typified by the resin structure in terms of present

Table 1 Percent uptake (%) of pertechnetate anion by PGME-deta samples at specific time intervals; standard error for percent uptake from triplicate measurements was ≤4.1%. (Part of data taken from Ref. [31])

Sample	1-deta			2-deta		
pH/time	90 (min)	180 (min)	24 (h)	90 (min)	180 (min)	24 (h)
1	93.5	98.4	98.7	83.4	91.5	98.1
2	92.0	98.3	99.1	82.5	91.6	98.0
3	91.7	98.3	99.3	80.7	92.3	97.9
4	90.9	98.1	99.7	81.0	93.1	97.4
5	90.3	97.5	99.1	80.2	91.7	97.6
6	90.1	96.2	98.6	79.1	92.1	97.0
7	87.9	94.9	98.3	79.5	91.4	96.4
8	86.4	95.3	96.4	77.4	92.5	94.1
9	84.2	92.0	93.1	76.5	91.0	91.2
10	56.3	70.3	83.2	54.3	67.7	82.1
11	29.5	48.3	72.1	27.5	44.5	70.7
12	15.8	20.0	62.0	15.0	22.2	60.3
13	3.6	4.6	6.9	2.8	5.0	8.2
14	5.4	3.5	5.3	2.7	3.5	6.1

functional groups, in this case amino groups. The sorption mechanism, that we propose for PGME copolymers grafted with diethylene triamine, is ion-pair formation in the diffuse double layer between NH_3^+ surface group, present under acidic and circumneutral conditions and $^{99m}TcO_4^-$ anions in solution [31].

The normal range for pH in surface water systems is 6.5–8.5 and for groundwater systems 6–8.5 [50]. Having this in mind, on the basis of the results presented in Table 1, and from the point of view of practical applications, it was concluded that the optimum pH value for sorption kinetics experiments would be 3.0. The maximum sorption capacity for shorter reaction times has a plateau in the pH range of 1.0–4.0, and the value of 3.0 was chosen so as to minimize the additional amount of chemicals that need to be added for the purpose of pH adjustment, while retaining the superior performance by both copolymer samples.

Kinetic models

Predicting the rate of the pollutants removal in a given solid/solution system is one of the most crucial factors for the effective design of sorption systems [51]. Adsorbate residence time and reactor dimensions are controlled by the system's kinetics [29] that is why it is very important to explore the sorption dynamics of the solute/sorbent system before utilization.

Table 2 shows sorption half-times and sorption capacities for two copolymers. After 24 h, both 1-deta and 2-deta sorb almost completely the pertechnetate present in the solution (99 and 98%, respectively), showing good potential for use in remediation strategies for slightly contaminated groundwater.

Adsorption mechanisms involving kinetics-based models have been reported in recent years [29]. Various kinetic models have described the reaction order of adsorption systems based on solution concentration (first- and second-order reversible, first- and second-order irreversible, and pseudo-first- and pseudo-second-order ones). On the other hand, kinetic models based on the sorption capacity on the solid phase have also been presented. These include Lagergren's first-order [52] or pseudo-first equation, Elovich [53], and Ho's pseudo-second-order expression [54].

The extent of our knowledge so far indicates that the sorption process consists of the four consecutive steps [54]: external mass transfer, boundary layer diffusion, intraparticle diffusion, and adsorption/desorption of solute molecules on/from the sorbent surface. The overall sorption rate may be controlled principally by one of these steps or any combination of them. The most widely used are models assuming that the surface reaction step controls the overall sorption rate [51]. Such models

Table 2 Sorption half time ($t_{1/2}$), capacities after 5 min (Q_5) and 30 min (Q_{30}), and maximum sorption capacities (Q_{max}) for pertechnetate sorption on amino-functionalized PGME samples

Sample	$t_{1/2}$ (min)	Q_5, MBq g^{-1} (%[a])	Q_{30}, MBq g^{-1} (%[a])	Q_{max}, MBq g^{-1} (%[a])
1-deta	21	6.06 (23)	16.8 (65)	25.8 (99)
2-deta	24	8.09 (31)	14.4 (56)	25.5 (98)

[a] Percent removal efficiency

include the pseudo-first, the pseudo-second order, and Elovich kinetic equations, which are currently among the most popular.

Probably the earliest known and one of the most widely used kinetic equations until now is Lagergren's pseudo-first order equation [52], which is usually not able to describe kinetic data as well as the pseudo-second order equation [55]. Nevertheless, there are examples to the contrary, although sparse [56, 57].

The pseudo-first order equation [52] is generally expressed as follows:

$$\log(Q_{\mathrm{eq}} - Q_t) = \log Q_{\mathrm{eq}} - \frac{(k_1 t)}{2.303} \tag{1}$$

where k_1 is the rate constant of pseudo-first-order sorption (min^{-1}), Q_{eq} and Q_t denote the amounts of sorbed pertechnetate anions at equilibrium and at time t (MBq g^{-1}), respectively. A plot of $\log(Q_{\mathrm{eq}} - Q_t)$ versus t should give a straight line to confirm the applicability of the kinetic model. In a true first-order process, $\log Q_{\mathrm{eq}}$ should be equal to the intercept of a plot of $\log(Q_{\mathrm{eq}} - Q_t)$ against t. The plot is shown in Fig. 3a.

The most commonly applied form of the pseudo-second order equation is given by Ho [54], and is expressed in its differential form as:

$$\frac{t}{Q_t} = \frac{1}{k_2 Q_{\mathrm{eq}}^2} + \frac{1}{Q_{\mathrm{eq}}} t \tag{2}$$

where k_2 (g^{-1} MBq^{-1} min^{-1}) is the rate constant of the pseudo-second order sorption, $h = k_2 Q_{\mathrm{eq}}^2$ is the initial rate constant (MBq g^{-1} min^{-1}). The values for the pseudo-second order reaction constants were derived from the regression analysis of t/Q_t versus t, (plot shown in Fig. 3b).

Contrary to the other models, the pseudo-second order model predicts the sorption behavior over the whole range of studies supporting a pseudo-second order equation and is in agreement with chemisorption being the rate-controlling step [58]. Chemisorption involves valency forces through the sharing or exchange of electrons between the adsorbent and adsorbate as covalent forces, as well as ion exchange. The advantage of using this model is that there is no need to know the equilibrium capacity from the experiments, as it can be calculated from the model. In addition, the initial adsorption rate can also be obtained from the model [29].

Elovich equation is also applied successfully to describe second-order kinetics, but this equation does not propose any definite mechanism for sorbate–sorbent reaction [53]. Due to the complexity of the original Elovich equation, it is most often used in its simplified form:

$$Q_t = \frac{\ln a_{\mathrm{e}} b_{\mathrm{e}}}{b_{\mathrm{e}}} + \frac{1}{b_{\mathrm{e}}} \ln t \tag{3}$$

where a_{e} is the initial adsorption rate (MBq g^{-1} min^{-1}) and the parameter b_{e} is related to the extent of surface coverage and activation energy for chemisorptions (g MBq^{-1}). The plot of Q_t versus ln t is shown in Fig. 3c.

The starting assumption is energetic heterogeneity of the actual solid surface. It has been widely accepted that the process of chemisorption can be described by this semi-empirical equation [59]. The non-physical behavior of the Elovich equation

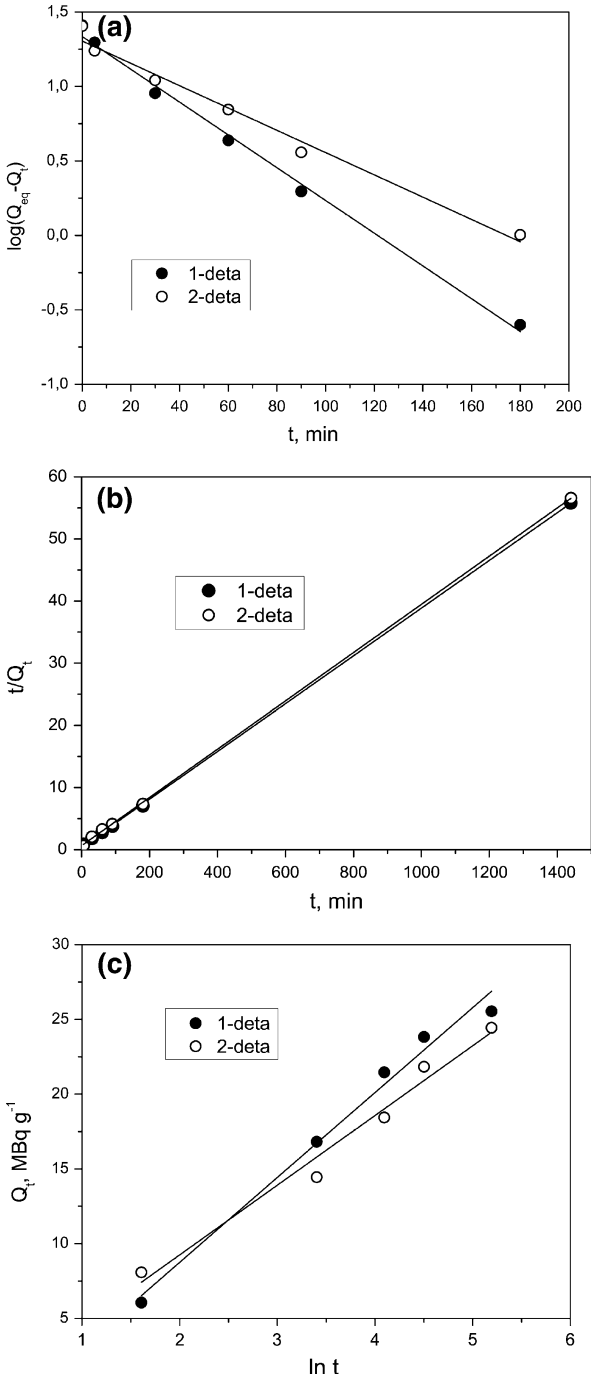

Fig. 3 Plots of Lagergren's first-order (**a**), pseudo-second-order (**b**), and Elovich (**c**) kinetic models for pertechnetate sorption for samples 1-deta (*black circles*) and 2-deta (*white circles*)

Table 3 Kinetic data for pertechnetate sorption on PGME-deta samples

Sample	Exp.	Models									
		Pseudo-first order			Pseudo-second order				Elovich		
	$Q_{e\ exp}$ (MBq g^{-1})	k_1 (min^{-1})	Q_e (MBq g^{-1})	R^2	k_2 (g MBq^{-1} $min^{-1)}$	Q_e (MBq g^{-1})	h (MBq g^{-1} min^{-1})	R^2	a_e (MBq g^{-1} min^{-1})	b_e (g MBq^{-1})	R^2
1-deta	25.8	0.0253	21.6	0.993	0.00328	26.0	2.22	0.999	3.59	0.176	0.981
2-deta	25.5	0.0173	20.2	0.981	0.00229	25.8	1.58	0.999	4.58	0.214	0.972

for longer adsorption times can be easily observed, i.e., $q(t \rightarrow \infty) = \infty$ [51]. According to the most of the theoretical interpretations, this is due to neglecting the rate of simultaneously occurring desorption. In practice, this restricts the applicability of the Elovich equation to the initial times of sorption process, when the system is relatively far from equilibrium. Both the pseudo-second order and the Elovich equations exhibit essentially identical behavior when considering the values of fractional surface coverage lower than about 0.7 [51].

The rate constants k_1, k_2, k_i, and h, the experimental equilibrium sorption capacity, $Q_{e,exp}$, the theoretical equilibrium sorption capacity, Q_e, and the correlation coefficients, R^2, calculated from the values of the intercepts and the slopes of the corresponding plots for the pseudo-first, the pseudo-second order, and the intraparticle diffusion equations are given in Table 3. Also, the R^2 values and the Elovich constants are provided in Table 3.

The correlation coefficients for the pseudo-second order model were equal to 0.999 for both investigated amino-functionalized copolymers (for the pseudo-first-order model, R^2 were equal to 0.993 and 0.981, for 1-deta and 2-deta, respectively), suggesting that the sorption of pertechnetate anion on 1-deta and 2-deta obeyed the pseudo-second-order kinetic model. $Q_{e,exp}$ and Q_e values obtained for the pseudo-second order model fit showed excellent agreement confirming this assumption, while that was not the case for the pseudo-first order model fit. The corresponding $Q_{e,exp}$ value for 1-deta was only slightly higher than that obtained for 2-deta. The relatively short $t_{1/2}$, as well as high Q_{max} values (Table 2), obtained for pertechnetate sorption on samples 1-deta and 2-deta suggests that both amino-functionalized samples can be regarded as efficient sorbents. Even though 1-deta has a significantly larger surface area, it has a lower content of amino groups that can interact with pertechnetate. The influence of different porous structures, although important, was not crucial, since pertechnetate sorption proceeds rapidly, especially during the first stage of sorption (up to 30 min). Namely, macroporous and super-macroporous structure provide high permeability, which is very favorable for sorption dynamics. In the context of the described sorption conditions, one should bear in mind that 370 MBq or 10 mCi of Tc-99m is approximately equal to 1.9×10^{-9} g, i.e., 1.9×10^{-11} mol. It is evident that the amino groups available for sorption of pertechnetate anion were present in large excess, in all the experiments.

To the best of our knowledge, the only attempt at modeling the kinetics of pertechnetate removal was by Chen and Veltkamp [21] who concluded that the loading process of pertechnetate onto 2-nitrophenyl octyl ether impregnated macroporous polymer followed the first-order kinetics. Yet, no other models were tested in this study.

The pseudo-first, the pseudo-second-order, and Elovich kinetic models are not able to identify the possible influence of the diffusion mechanism, so the results were analyzed using the Bangham and the intraparticle diffusion models, having in mind that both PGME-deta samples have a well developed macroporous structure. The effect of intraparticle diffusion on sorption rate was obtained from the treatment of the collected data according to the following intraparticle diffusion model [60]:

$$Q_t = x + k_i t^{0.5} \tag{4}$$

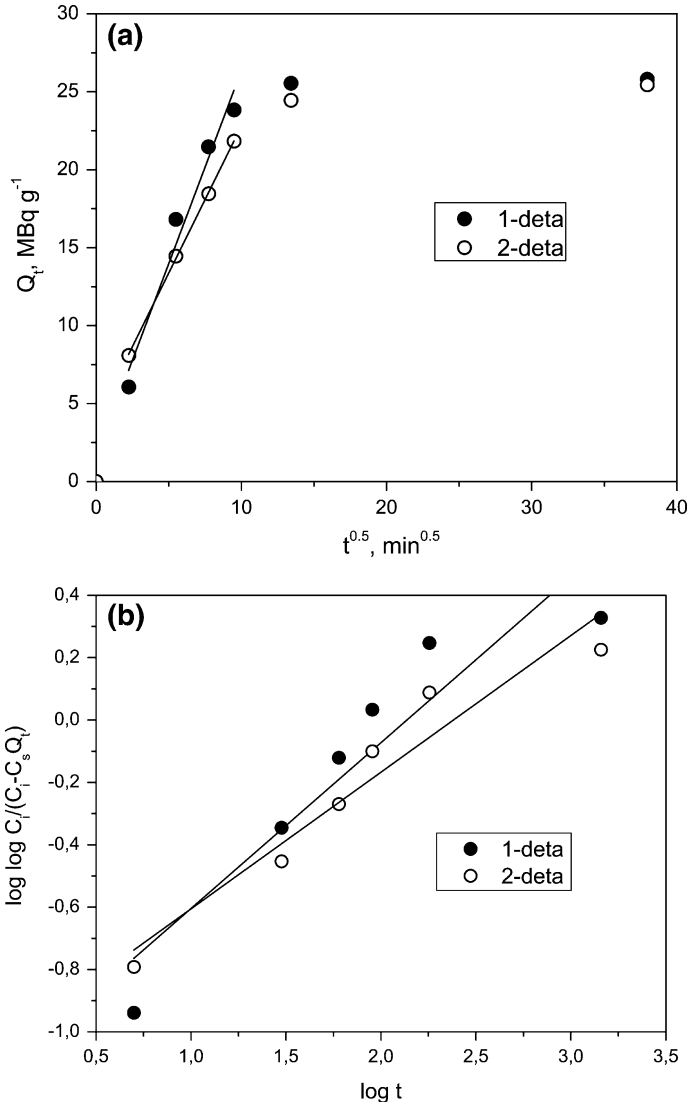

Fig. 4 Intraparticle and Bangham diffusion modeling of pertechnetate sorption on PGME-deta samples [1-deta (*black circles*], 2-deta (*white circles*)]

where k_i (MBq g^{-1} min$^{-0.5}$) is the intraparticle diffusion rate constant and x is the intercept which is proportional to the boundary layer thickness. A linear plot of Q_t versus $t^{0.5}$ which passes through the origin indicates that intraparticle diffusion is a rate-controlling step in the sorption process [61]. When the plots do not pass through the origin, this is indicative of some degree of boundary layer control. Also, the plot of our data of Q_t versus $t^{0.5}$ for pertechnetate sorption on PGME-deta samples, which is shown in Fig. 4a, is of a double nature, i.e., two components are found in the form of

Table 4 Kinetic data for intraparticle and Bangham diffusion models

Samples	x (MBq g^{-1})	k_{id} (MBq g^{-1} min$^{-0.5}$)	R^2
Intraparticle diffusion			
1-deta	1.59	2.48	0.952
2-deta	3.94	1.88	0.999
	$k_b \times 10^3$ (g^{-1})	α	R^2
Bangham diffusion			
1-deta	0.0541	0.532	0.847
2-deta	0.0663	0.438	0.924

two straight lines which confirms that intraparticle diffusion is not a fully operative mechanism for this system [62]. Kinetic data for the intraparticle diffusion model is shown in Table 4.

When researching adsorption of metal ions on inorganic porous materials, Gupta and Bhattacharyya [63] came to a conclusion that while the main mechanism of adsorption of metal ions on various inorganic solids may be mostly second order and occasionally first order, the initial uptake always has a strong presence of intraparticle diffusion.

Kinetic data were further used to confirm the influence of pore diffusion occurring in the present adsorption system using Bangham's equation [64] which is commonly expressed as:

$$\log\log\left[\frac{C_0}{C_0 - C_s Q_t}\right] = \log\left[\frac{k_b C_s}{2.303V}\right] + \alpha \log t \tag{5}$$

where C_0 is the initial concentration of sorbate in the solution (MBq dm^{-3}), V is the volume of the solution (dm^{-3}), C_s is the dosage of sorbent (g dm^{-3}), Q_t denotes the amounts of sorbed pertechnetate anions at time t (MBq g^{-1}), α (<1) and k_b are constants, which are calculated from the intercept and the slope of the straight line plots of $\log\log[C_0/(C_0 - C_s Q_t)]$ versus $\log t$. If this equation is an adequate representation of the experimental data, then the adsorption kinetics are limited by pore diffusion. The double logarithmic plots according to above equation, shown in Fig. 4b, did not yield linear curves showing that the diffusion of adsorbate into the pores of the sorbent is not the only rate-controlling step [65]. The Bangham model kinetic data is shown in Table 4. The higher R^2 for sample 2-deta will suggest that the contribution of pore diffusion in the sorption of pertechnetate onto PGME-deta is higher than this sample than for 1-deta, which could be attributed to the lower surface area of 2-deta [66].

Conclusion

Two samples of macroporous crosslinked poly(glycidyl methacrylate-*co*-ethylene glycol dimethacrylate), PGME, with different amounts of the crosslinker and different porosity parameters, were functionalized by the ring-opening reaction of

epoxy groups with diethylene triamine (abbreviated PGME-deta) and used for pertechnetate ($^{99m}TcO_4^-$) sorption. Sorption kinetic study showed that the pertechnetate sorption by PGME-deta obeys the pseudo-second-order kinetic model. The positive intercepts of the intraparticle diffusion plots indicated some degree of boundary layer control, while their shape confirmed the influence of intraparticle diffusion on sorption rates. Bangham plot confirmed that the pore diffusion was not the only rate-limiting process. The optimum pH value for $^{99m}TcO_4^-$ sorption chosen for kinetic study was 3.0, with relatively low sorption half time of around 20 min, and maximum sorption capacities of around 25 MBq g^{-1}. After 24 h, both samples 1-deta and 2-deta sorbed almost completely the pertechnetate present in the solution (99 and 98%, respectively), showing good potential for use in remediation strategies.

Acknowledgment This study was supported by the Ministry of Education and Science of the Republic of Serbia (Projects No. III 43009, III 45001 and ON 172018).

References

1. Schwochau K (2000) Artificial occurrence. In: Technetium: chemistry and radiopharmaceutical applications, 1st edn. Wiley-VCH, New York, pp 10–34
2. Garcia-Leon M (2005) ^{99}Tc in the environment: sources, distribution and methods. J Nucl Radiochem Sci 6(3):253–259
3. Rard JA, Rand MH, Anderegg G, Wanner H (1999) Discussion of data selection. In: Sandino MCA, Östhols E (eds) Chemical thermodynamics 3: chemical thermodynamics of technetium. Elsevier Science, North-Holland, pp 63–266
4. Winkler A, Brühl H, Trapp C, Bock WD (1998) Mobility of technetium in various rock and defined combinations of natural minerals. Radiochim Acta 44(45):183–186
5. Wharton MJ, Atkins B, Charnock JM, Livens FR, Pattrick RAD, Colison D (2000) An X-ray absorption spectroscopy study of the coprecipitation of Tc and Re with Mackinawite (FeS). Appl Geochem 15:347–354
6. USEPA, U.S. Environmental Protection Agency, Office of Air and Radiation (2004) Contaminant geochemistry and K_d values. In: Understanding variation in partition coefficient, K_d, values, volume III: review of geochemistry and available K_d values for Americium, Arsenic, Curium, Iodine, Neptunium, Radium, and Technetium. EPA 402-R-04-002C. http://www.epa.gov/radiation/docs/kdreport/vol3/402-r-04-002c.pdf. Accessed 13 June 2011
7. Yoshihara K (1996) Technetium in the environment. Top Curr Chem 176:17–35
8. Amano R, Ando A, Hiraki T, Mori H, Matsuda H, Hisada K (1990) Rapid uptake of technetium-99m pertechnetate by several plants. Radioisotopes 39:583–586
9. USEPA (2002) EPA facts about technetium-99. http://www.epa.gov/superfund/health/contaminants/radiation/pdfs/technetium.pdf. Accessed 13 June 2011
10. Peretroukhine V, Sergeant C, Devès G, Poulain S, Vesvres MH, Thomas B, Simonoff M (2005) Technetium sorption by stibnite from natural water. Radiochim Acta 94(9–11):665–669
11. Lieser KH, Bauscher CH (1988) Technetium in the hydrosphere and in the geosphere. II. Influence of pH, of complexing agents and of some minerals on the sorption of technetium. Radiochim Acta 44(45):125–128
12. Cul GD, del Bostick WD, Trotter DR, Osborne PE (1993) Technetium-99 removal from process solutions and contaminated groundwater. Sep Sci Technol 28:551–564
13. Bors J, Dultz S, Riebe B (2000) Organophilic bentonites as adsorbents for radionuclides I. Adsorption of ionic fission products. Appl Clay Sci 16:1–13
14. Gu B, Dowlen KE, Liang L, Clausen JL (1996) Efficient separation and recovery of technetium-99 from contaminated groundwater. Sep Technol 6:123–132

15. Wang Y, Gao H, Yeredla R, Xu H, Abrecht M (2007) Control of pertechnetate sorption on activated carbon by surface functional groups. J Colloid Interface Sci 305:209–217
16. Holm E, Gäfvert T, Lindahl P, Roos P (2000) In situ sorption of technetium using activated carbon. Appl Radiat Isot 53:153–157
17. Liang L, Gu B, Yin X (1996) Removal of technetium-99 from contaminated groundwater with sorbents and reductive materials. Sep Technol 6:111–112
18. Chen QJ, Dahlgaard H, Hansen HJM, Aarkrog A (1990) Determination of 99Tc in environmental samples by anion exchange and liquid–liquid extraction at controlled valency. Anal Chim Acta 228:163–167
19. Suzuki T, Fujii Y, Yan W, Mimura H, Koyama S, Ozawa M (2009) Adsorption behavior of VII group elements on tertiary pyridine resin in hydrochloric acid solution. J Radioanal Nucl Chem 282:641–644
20. Bonnesen PV, Brown GM, Alexandratos S, Bavoux LB, Presley DJ, Patel V, Ober R, Moyer BA (2000) Development of bifunctional anion exchange resins with improved selectivity and sorptive kinetics for pertechnetate. Batch-equilibrium experiments. Environ Sci Technol 34:3761–3766
21. Chen J, Veltkamp JC (2002) Pertechnetate removal by macroporous polymer impregnated with 2-nitrophenyl octyl ether (NPOE). Solvent Extr Ion Exch 20:515–524
22. Katayev EA, Kolesnikov GV, Sessler JL (2009) Molecular recognition of pertechnetate and perrhenate. Chem Soc Rev 38:1572–1586
23. Nastasović A, Sandić Z, Suručić Lj, Maksin D, Jakovljević D, Onjia A (2009) Kinetics of hexavalent chromium sorption on amino-functionalized macroporous glycidyl methacrylate copolymer. J Hazard Mater 171(1–3):153–159
24. Kalalova E, Thuy P (1990) Separation of iridium from platinum using a modified glycidyl methacrylate copolymer with diethylamino groups. Angew Makromol Chem 180:159–167
25. Bicak N, Sherrington DC, Sungur S, Tan N (2003) A glycidyl methacrylate-based resin with pendant urea groups as a high capacity mercury specific sorbent. React Funct Polym 54:141–147
26. Kim E, Benedetti MF, Boulègue J (2004) Removal of dissolved rhenium by sorption onto organic polymers: study of rhenium as an analogue of radioactive technetium. Water Res 38:448–454
27. Plevaka AV, Troshkina ID, Zemskova LA, Voit AV (2009) Rhenium sorption by fibrous chitosan-carbon materials. Russ J Inorg Chem 54(7):1168–1171
28. USEPA (1995) Dynaphore, Inc. Forager™ Sponge Technology Innovative Tecnology Evaluation Report 540/R-94/522a. http://www.epa.gov/nrmrl/lrpcd/site/reports/540r94522/540r94522.pdf. Accessed 13 June 2011
29. Ho YS (2006) Review of second-order models for adsorption systems. J Hazard Mater B136:681–689
30. Knoll G (1979) Radiation detection and measurement. Wiley, Hoboken, NJ
31. Hercigonja RV, Maksin DD, Nastasović AB, Trifunović SS, Glodić PB, Onjia AE (2011) Adsorptive removal of technetium-99 using macroporous poly(GMA-co-EGDMA) modified with diethylene triamine. J Appl Polym Sci. doi: 10.1002/app.34693
32. Švec F, Fréchet JMJ (1995) Temperature, a simple and efficient tool for the control of pore size distribution in macroporous polymers. Macromolecules 28:7580–7582
33. Paredes B, González S, Rendueles M, Villa-García MA, Díaz M (2003) Influence of the amination conditions on the textural properties and chromatographic behaviour of amino-functionalized glycidyl methacrylate-based particulate supports. Acta Mater 51:6189–6198
34. Webb PA, Orr C (1997) Analytical methods in fine particle technology. Micrometrics Instrument Corporation, Norcross, GA
35. Darab JG, Amonette AB, Burke DSD, Orr RD (2007) Removal of pertechnetate from simulated nuclear waste streams using supported zerovalent iron. Chem Mater 19:5703–5713
36. Westinghouse Hanford Co (1994) Report WHC-SD-WM-RD-044. http://www.osti.gov/bridge/servlets/purl/10148288-GkWAwl/native/10148288.pdf. Accessed 12 September 2011
37. IAEA (1994) Classification of radioactive waste: a safety guide. Safety series No. 111-G-l.l International Atomic Energy Agency, Vienna
38. Bond AH, Chang FWK, Thakkar AH, Williamson JM, Gula MJ, Harvey JT, Griffin ST, Rogers RD, Horwitz EP (1999) Design, synthesis, and uptake performance of ABEC resins for the removal of pertechnetate from alkaline radioactive wastes. Ind Eng Chem Res 38:1676–1682
39. Anderson H, Asprey L (1960) Solvent extraction process for plutonium. US patent 2924506
40. Rard JA (2005) Current status of the thermodynamic data for technetium and its compounds and aqueous species. J Nucl Radiochem Sci 6:197–204

41. Um W, Chang HS, Icenhower JP, Lukens WW, Serne RJ, Qafoku NP, Westsik JH Jr, Buck EC, Smith SC (2011) Immobilization of 99-technetium (VII) by Fe(II)-goethite and limited reoxidation. Environ Sci Technol 45:4904–4913
42. Wildung RE, McFadden KM, Garland TR (1979) Technetium sources and behaviour in the environment. J Environ Qual 8:156–161
43. IAEA (2002) Application of ion exchange processes for the treatment of radioactive waste and management of spent ion exchangers, technical reports series No. 408. IAEA, Vienna
44. USEPA (1981) U.S. Environmental Protection Agency. Summary report: control and treatment technology for the metal finishing industry-ion exchange. USEPA EPA 625/-81-007
45. Diamond RM, Whitney DC (1966) Resin selectivity in dilute to concentrated aqueous solutions. In: Marinsky J (ed) Ion exchange, a series of advances, vol 1. Marcel Dekker, New York, pp 277–351
46. Gregor HP, Belle J, Marcus RA (1955) Studies on ion-exchange resins. XIII. Selectivity coefficients of quaternary base anion-exchange resins toward univalent anions. J Am Chem Soc 77:2713–2719
47. Piracha A, Zulfiqar S, McNeill IC (1996) The thermal degradation of copolymers of glycidyl methacrylate and vinylacetate. Polym Degrad Stab 51:319–326
48. Çaykara T, Çakar F, Demirci S (2008) A new type of poly(glycidyl methacrylate) microbeads with surface grafted iminodiacetic acid: synthesis and characterization. Polym Bull 61:311–318
49. Koopal LK, van Riemsdijk WH, de Wit JCM, Benedetti MF (1994) Analytical isotherm equations for multicomponent adsorption to heterogeneous surfaces. J Colloid Interface Sci 166:51–60
50. Oram B (2011) The pH of water. Water Research Center. http://www.water-research.net/ph.htm. Accessed on 11 September 2011
51. Plazinski W, Rudzinski W, Plazinska A (2009) Theoretical models of sorption kinetics including a surface reaction mechanism: a review. Adv Colloid Interface Sci 152:2–13
52. Lagergren S (1898) About the theory of so-called adsorption of soluble substances. ***K Sven Vetenskapsakad Handl 24:1–39
53. Sparks DL (1989) Kinetics of soil chemical processes. Academic Press Inc., New York
54. Ho YS, Ng JCY, McKay G (2000) Kinetics of pollutant sorption by biosorbents: review. Sep Purif Methods 29:189–232
55. Febrianto J, Kosasih AN, Sunarso J, Ju Y, Indraswati N, Ismadji S (2009) Equilibrium and kinetic studies in adsorption of heavy metals using biosorbent: a summary of recent studies. J Hazard Mater 162:616–645
56. Janoš P, Michálek P, Turek L (2007) Sorption of ionic dyes onto untreated low-rank coal–oxihumolite: a kinetic study. Dyes Pigment 74:363–370
57. Lin CC, Lai Y (2006) Adsorption and recovery of lead(II) from aqueous solutions by immobilized Pseudomonas Aeruginosa PU21 beads. J Hazard Mater 137:99–105
58. Ho YS, McKay G (1998) A comparison of chemisorption kinetic models applied to pollutant removal on various sorbents. Process Saf Environ Prot (Trans Ichem E, B) 76(4):332–340
59. Zhang J, Stanforth R (2005) Slow adsorption reaction between arsenic species and Goethite (α-FeOOH): diffusion or heterogeneous surface reaction control. Langmuir 21:2895–2901
60. Boyd GE, Adamson AW, Myers LS (1947) The exchange adsorption of ions from aqueous solutions by organic zeolites, II: kinetics. J Am Chem Soc 69:2836–2842
61. Özcan A, Özcan AS (2005) Adsorption of acid Red 57 from aqueous solutions onto surfactant-modified sepiolite. J Hazard Mater B125:252–259
62. Singh S, Rai BN, Rai LC (2001) Ni(II) and Cr(VI) sorption kinetics by *Mycrocystis* in single and multimetallic system. Process Biochem 36:1205–1212
63. Gupta SS, Bhattacharyya KG (2011) Kinetics of adsorption of metal ions on inorganic materials: a review. Adv Colloid Interface Sci 162:39–58
64. Aharoni C, Ungarish M (1977) Kinetics of activated chemisorptions: part 2. Theoretical models. J Chem Soc Faraday Trans 73:456–464
65. Tutem E, Apak R, Unal CF (1998) Adsorptive removal of chlorophenols from water by bituminous shale. Water Res 32(8):2315–2324
66. Ofomaja AE, Naidoo EB, Modise SJ (2010) Kinetic and pseudo-second-order modeling of lead biosorption onto pine cone powder. Ind Eng Chem Res 49:2562–2572